

# $J/\psi$ suppression at forward rapidity as a potential probe for QGP formation in colour screening scenario

M. Mishra<sup>1</sup>, C. P. Singh<sup>2</sup> and V. J. Menon

*Department of Physics, Banaras Hindu University, Varanasi 221005, India*

## Abstract

In order to study the properties of  $J/\psi$  in the deconfining medium, we extend our previous formalism [Phys. Lett. B **656** (2007) 45] on  $J/\psi$  suppression at mid-rapidity using the colour screening framework. Our formalism is more general as the complete rapidity and centrality dependence including  $J/\psi$  suppression at forward as well as mid-rapidity can be computed directly from it. Careful attention is paid to the role of the medium's proper time in determining the locus of the deadly region where  $J/\psi$  gets killed. Other important ingredients in the calculation are bag model equation of state for QGP, the longitudinal expansion of the QGP fluid obeying Bjorken's boost invariant scaling law and non-sequential/sequential melting of  $\chi_c$  (1P) as well as  $\psi'$  (2S) higher resonances. Upon comparison with the recent data of PHENIX collaboration on  $J/\psi$  suppression at forward and mid-rapidity regions, we find that our model shows a reasonable agreement with the data. Furthermore, we observe a larger suppression at forward rapidity in our model which is again well supported by the PHENIX data.

**PACS numbers:** 25.75.-q; 25.75.Nq; 12.38.Mh; 25.75.Gz

**Keywords:**  $J/\psi$  suppression; survival probability; sequential melting; relativistic heavy-ion collisions; colour Debye screening; general rapidity.

---

<sup>1</sup>Email: madhukar.12@gmail.com

<sup>2</sup>Email: cpsingh\_bhu@yahoo.co.in

# 1 Introduction

The current experimental programmes at RHIC are focused towards the investigations of the properties of hadrons or hadronic resonances above the deconfinement transition. In particular, suppression of  $J/\psi$  (or charmonium state) has been suggested as a potential probe of the deconfined matter produced in the ultra-relativistic heavy-ion collisions. Lattice quantum chromodynamics (QCD) calculations reveal that the critical temperature for confined normal nuclear matter (HG) to deconfined matter (QGP) phase transition is  $T_c \sim 0.160 - 0.190$  GeV if a baryonic chemical potential  $\mu_B = 0$  [1] although there are controversies whether such a transition is of first order or only crossover [2, 3]. Matsui and Satz [4] first predicted that the binding potential of the  $c\bar{c}$  pair into  $J/\psi$  mesons is screened in the presence of a QGP medium and  $J/\psi$  states dissociate at temperatures for which the colour (Debye) screening radius of the medium falls below their corresponding  $c\bar{c}$  binding radius. The strength of the suppression depends on the binding energies of the quarkonia and the temperature of the medium [4]. Old lattice QCD simulations [5, 6] suggested that the  $J/\psi$  could survive in QGP up to dissociation temperature  $T_D \sim 2.1T_c$  and the higher resonances, such as  $\chi_c$  (1P) and  $\psi'$  can still melt near  $T_c$ , however new QCD analysis [7] shows that the dissociation temperatures of all the relevant quarkonia viz  $J/\psi$ ,  $\chi_c$ , and  $\psi'$  are close to  $T_c$ . The  $J/\psi$  and their higher resonances are created at the initial (pre-thermal) stage of heavy-ion collisions because of their large masses. Their small widths also make them insensitive to final state interactions. Therefore,  $J/\psi$  quarkonia can probe the evolution of the deconfined state of matter from the early stage of collisions [8].

There are now high-statistics data available on the  $J/\psi$  suppression obtained by NA50 experiments [9, 10, 11] at SPS and by PHENIX experiments at RHIC [12]. One of the surprising result is the observation of a similar suppression pattern at both these energies involving a large difference in the energy densities produced between SPS and RHIC. The other important feature of the PHENIX  $J/\psi$  suppression data from Au+Au collisions at the center-of-mass energy  $\sqrt{s_{NN}} = 200$  GeV at RHIC is that  $J/\psi$  yield in the central Au+Au collisions is suppressed by a factor of nearly 4 at mid-rapidity and 5 at forward rapidity as compared to that in p+p collisions scaled by the average number of binary collisions. The absolute suppression of  $J/\psi$  in heavy-ion collisions can arise due to initial state effects (e.g., cold nuclear matter effects) and/or final state effects (e.g., colour screening, due to possible formation of hot QGP). Two types of models have been proposed in order to explain the above results. In first type of models, one considers that  $\chi_c$  (1P) and  $\psi'$  (2S) states evaporate shortly above  $T_c$  while  $J/\psi$  (1S) will do so if the temperature rises above  $2.1T_c$  or  $1.2T_c$  according to old [6] and new [7] estimates, respectively. In second type of models, it is assumed that  $J/\psi$  yield will result from a balance between annihilation of  $J/\psi$  due to thermal gluons [13, 14] along with colour screening [15, 16] and enhancement due to coalescence of uncorrelated  $c\bar{c}$  pairs [17, 18, 19] which are produced abundantly at RHIC energy [20, 21]. However, PHENIX data do not show any indication of  $J/\psi$  enhancement.

*Cold nuclear matter (CNM)* effects such as nuclear absorption, shadowing and anti-shadowing are also expected to modify the  $J/\psi$  yield. CNM effects due to the gluon shadowing and nuclear absorption of  $J/\psi$  at the RHIC energy were evaluated from the  $J/\psi$  measurement in d+Au collisions at RHIC [22, 23]. PHENIX data on the centrality depen-

dence of  $J/\psi$  suppression have already been analyzed in several models such as comover model [24], statistical coalescence model [25, 26], kinetic model [17], statistical hadronization model [27] and QCD based nuclear absorption model [28]. None of these models gives a satisfactory description of the present experimental data. In particular, we do not find any single mechanism which can be used to explain the complete rapidity dependence of the  $J/\psi$  suppression. Chaudhuri has attempted to explain the suppression at forward-rapidity [29] in a QGP motivated threshold model supplemented with normal nuclear absorption. However, this appears more like a parameter fitting because the parameters used in the analysis (e.g., QGP formation time  $\tau = 0.06 - 0.08$  fm/c) do not convey any physical meaning. Moreover, in order to accommodate rapidity dependence in the formulation, he considers three parameters used in the analysis e.g.,  $J/\psi$  nuclear absorption cross-section, threshold density and its smearing factor  $\lambda$  to explicitly depend on the rapidity variable. Similarly Gunji et al. [30] have recently used a hydro+ $J/\psi$  model in which QGP has been considered as undergoing (3+1)-dimensional hydrodynamic expansion but it has been used to explain the mid-rapidity data only without incorporating  $J/\psi$  formation time. Recently, we analyzed [15] the mid-rapidity PHENIX data of  $J/\psi$  suppression, normalized by contribution due to cold nuclear matter effects [30, 31, 32], using a modified colour screening model of Chu and Matsui [16]. Moreover, we had taken a bag model equation of state, (1+1)-dimensional hydrodynamic evolution for QGP as well as additional time dilatation effect for charmonium as other ingredients in our model. We found that the model described the centrality dependence of  $J/\psi$  suppression at mid-rapidity quite well [15].

In this paper, we generalize the above geometric formulation in order to incorporate the rapidity dependence by explicitly introducing rapidity variable in a consistent manner. Here again we consider (1+1)-dimensional hydrodynamic evolution of the QGP and the possible sequential dissociation scenario [31] for the charmonium excited states. Our theory emphasizes the role of the medium's proper time in finding the locus of the deadly region and also shows how this locus explicitly depends on the  $J/\psi$  rapidity. We predict the centrality (i.e., impact parameter or number of participant nucleons  $N_{part}$ ) dependence of the  $J/\psi$  suppression in Au+Au collisions at mid-rapidity as well as at forward rapidity and compare with the experimental data reported recently by PHENIX collaboration at RHIC. We notice that our model reproduces the main features of the data quite well. We also find that the present model gives more  $J/\psi$  suppression at forward rapidity than that at mid-rapidity and this fact is again in quite good agreement with the recent PHENIX data. Results are reported corresponding to old [6] and new [7] values of the dissociation temperatures of the quarkonia.

## 2 Formulation

Although our basic theme is similar to that described in refs. [15, 16, 33], yet for the sake of convenience, we briefly recapitulate it below and also point out the important differences at appropriate places. For a QGP with massless quarks and gluons, the bag model EOS gives [15, 34]:

$$\epsilon = aT^4/c_s^2 + B \quad ; \quad P = aT^4 - B \sim a(T^4 - T_c^4); \quad (1)$$

$$c_s^2 \equiv \frac{\partial P}{\partial \epsilon} \quad ; \quad a \equiv \frac{37\pi^2}{90} \quad ; \quad B \equiv \frac{17\pi^2 T_c^4}{45} \sim a T_c^4,$$

where at every time-space point  $x \equiv (t, \vec{x})$ ,  $\epsilon$  is the energy density,  $P$  the pressure,  $T_c$  the critical temperature,  $c_s^2$  the square of velocity of sound, the coefficient  $a$  describes the number of degrees of freedom, and  $B$  is the bag constant. It should be added here that the bag model EOS exhibits a first order phase transition between the QGP and the HG phases which is not well supported by the recent lattice QCD simulations [2, 3]. Even though the bag model EOS has often been used for hydrodynamic calculations, it should be understood as a convenient way of parameterizing some features of the EOS with a rapid change of entropy density as a function of temperature in the transition region. For a QGP undergoing (1+1)-dimensional Bjorken's boost invariant expansion, the local thermodynamic observables become function of the lateral coordinate  $r$  along with the proper time  $\tau \equiv (t^2 - z^2)^{1/2}$ , so that the cooling laws become

$$\tilde{\epsilon} \equiv \tilde{P} = \tilde{T}^4 = \tilde{\tau}^{-q} \quad ; \quad q \equiv 1 + c_s^2, \quad (2)$$

where the dimensionless symbols  $\tilde{\tau} \equiv \tau/\tau_i$ ,  $\tilde{T} \equiv T(\tau, r)/T(\tau_i, r)$ ,  $\tilde{\epsilon} \equiv (\epsilon(\tau, r) - B)/(\epsilon(\tau_i, r) - B)$  and  $\tilde{P} \equiv (P(\tau, r) + B)/(P(\tau_i, r) + B)$ , have been introduced for convenience with  $\tau_i$  being the proper time for initial thermalization of the fireball.

From (1) the pressure is seen to almost vanish at the transition point  $T_c$ , i.e., in the hadronic sector. Hence on any transverse plane we choose the initial pressure profile

$$P(\tau_i, r) = P(\tau_i, 0) h(r) \quad ; \quad h(r) \equiv \left(1 - \frac{r^2}{R_T^2}\right)^\beta \theta(R_T - r), \quad (3)$$

where  $R_T$  denotes the radius of the cylinder. The power  $\beta$  depends on the energy deposition mechanism, and  $\theta$  is the unit step function. Clearly, our pressure is maximum at the center of the plasma but vanishes at the edge  $R_T$  where hadronization occurs. The factor  $P(\tau_i, 0)$  is related to the mean pressure  $\langle P \rangle_i$  over the cross-section and to the corresponding average initial energy density  $\langle \epsilon \rangle_i$  via

$$P(\tau_i, 0) = (1 + \beta) \langle P \rangle_i = (1 + \beta) \{c_s^2 \langle \epsilon \rangle_i - q B\}. \quad (4)$$

In the present work, we take the initial average energy density  $\langle \epsilon \rangle_i$  in terms of the number of participating nucleons  $N_{part}$  [31] (which in turn depends on the impact parameter  $b$ ), given by the modified Bjorken formula:

$$\langle \epsilon \rangle_i = \frac{\xi}{A_T \tau_i} \left( \frac{dE_T}{dy_H} \right)_{y_H=0} \quad ; \quad A_T = \pi R_T^2, \quad (5)$$

where  $A_T$  is the transverse overlap area of the colliding nuclei and  $(dE_T/dy_H)_{y_H=0}$  is the transverse energy deposited per unit rapidity of output hadrons. Both depend on the number of participants  $N_{part}$  [35] and thus provide centrality dependent initial average energy density  $\langle \epsilon \rangle_i$  in the transverse plane. The phenomenological scaling factor  $\xi$  discussed latter in Sec. 3 in conjunction with the self-screened parton cascade model.

It is well known that  $c\bar{c}$  bound state in a thermal medium feels a colour screened Yukawa potential and it melts at the dissociation temperature  $T_D$  (determined by recent Lattice QCD simulations [6, 7]) which corresponds to the energy density  $\epsilon_s$  and pressure  $P_s$  given by

$$T_D \geq T_c \quad ; \quad \epsilon_s = a T_D^4 / c_s^2 + B \quad ; \quad P_s = a T_D^4 - B. \quad (6)$$

For any chosen fireball instant  $t$  and on the arbitrary  $z$  plane the contour of constant pressure  $P_s$  is obtained by combining the cooling laws (3) with the profile shape (4) to yield

$$\tilde{P} \equiv \frac{P_s + B}{P(\tau_i, 0) h(r) + B} = \tilde{\tau}^{-q}. \quad (7)$$

Setting  $r = 0$  the maximum allowed tilde time  $\tilde{\tau}_{s0}$  (during which pressure drops to  $P_s$  at the center) can be identified as

$$\tilde{\tau}_{s0} \equiv \left\{ \frac{P(\tau_i, 0) + B}{P_s + B} \right\}^{1/q}, \quad (8)$$

with  $P(\tau_i, 0)$  read-off from (4). Thereby the said locus takes the more convenient form

$$\left( 1 - \frac{r^2}{R_T^2} \right)^\beta = H_s(\tau) \equiv \frac{\tilde{\tau}^q - B/(P_s + B)}{\tilde{\tau}_{s0}^q - B/(P_s + B)}. \quad (9)$$

Our above result generalizes a similar expression derived by us [15] for the special case when the transverse plane passes through the origin and the proper time was  $t$  itself.

Next, consider an interacting  $c\bar{c}$  pair created at the early time  $t_1 \sim \hbar/2m_c \approx 0$  at the location  $(r_1, \phi_1, z_1)$  inside a cylinder of length  $L_1$ . The precise value of  $L_1$  is not known a priori since different physical arguments can give different results, among which a recipe exploiting rapidity will turn out to be logical as discussed in the numerical section. The  $c\bar{c}$  pair has mass  $m$ , transverse momentum  $p_T$ , transverse mass  $m_T = \sqrt{m^2 + p_T^2}$ , rapidity  $y$ , total energy  $p^0 = m_T \cosh(y)$ , longitudinal momentum  $p_z = m_T \sinh(y)$ , vectorial velocity  $\vec{v} = (\vec{p}_T + \vec{p}_z)/p^0$  and dilation factor  $\gamma = p^0/m$ . In the fireball frame the pair will convert itself into the physical  $J/\psi$  resonance after the lapse of time  $t = \gamma \tau_F$  (with  $\tau_F$  being the intrinsic formation time) provided the temperature  $T < T_D$ . At this instant the pair's transverse position  $\vec{r}$ , its longitudinal position  $z$  and medium's proper time  $\tau$  are given by

$$\begin{aligned} \vec{r} &= \vec{r}_1 + v_T t \quad ; \quad z = z_1 + v_z t \\ \tau &= (t^2 - z^2)^{1/2} \theta(t - |z|) \quad ; \quad t \equiv \gamma \tau_F. \end{aligned} \quad (10)$$

From the locus (9) we deduce the so called screening radius

$$r_s = R_T \{1 - H_s^{1/\beta}(\tau)\}^{1/2} \theta\{1 - H_s(\tau)\}. \quad (11)$$

In contrast to the earlier paper [15], the important role of proper time  $\tau$  and hence of the longitudinal velocity  $v_z$  must be noted in the definition of the screening radius  $r_s$ , which marks the boundary of the circular region where the quarkonium formation is prohibited. Since  $\tau$  and hence  $H_s(\tau)$  decreases as  $|v_z|$  increases, it is clear that the radius  $r_s$  of the

deadly region grows with growing rapidity. This fact will be utilized for interpreting our graphical results in Sec. 4.

Due to the existence of the deadly region the pair will escape and form quarkonium if  $|\vec{r}_1 + \vec{v}_T t| \geq r_s$  implying

$$\cos(\phi_1) \geq Y \quad ; \quad Y \equiv \frac{[(r_s^2 - r_1^2) - v_T^2 t^2]}{2 r_1 t |v_T|}, \quad (12)$$

where the roll of the transverse velocity  $v_T$  has become explicit. This trigonometric inequality is equivalent to saying that  $-\phi_{max}(r_1, z_1) \leq \phi_1 \leq \phi_{max}(r_1, z_1)$  where

$$\phi_{max}(r_1, z_1) = \begin{cases} \pi & \text{if } Y \leq -1, \\ \pi - \cos^{-1} |Y| & \text{if } -1 \leq Y \leq 0, \\ \cos^{-1} |Y| & \text{if } 0 \leq Y \leq 1, \\ 0 & \text{if } Y \geq 1. \end{cases}$$

In contrast to our earlier work [15] the symbol  $\phi_{max}$  depends on both  $r_1$  and  $z_1$ .

Finally, we must deal with the anomalous survival probability due to QGP effect namely,  $S(N_{part}, p_T, y)$ . Suppose the overall probability distribution for the production of  $c\bar{c}$  pair at general position with general momentum is factorized as  $P \propto f(r_1) g(p_T, y)$ , where the radial profile function is

$$f(r_1) \propto \left(1 - \frac{r_1^2}{R_T^2}\right)^\alpha \theta(R_T - r_1), \quad (13)$$

with  $\alpha = 0.5$  [16] and the momentum distribution  $g(p_T, y)$  is left unspecified because it cancels out from the expression of the net survival probability in colour screening scenario defined by

$$S = \frac{\int_0^{R_T} dr_1 r_1 f(r_1) \int_{-L_1/2}^{L_1/2} dz_1 \int_{-\phi_{max}}^{\phi_{max}} d\phi_1}{\int_0^{R_T} dr_1 r_1 f(r_1) \int_{-L_1/2}^{L_1/2} dz_1 \int_{-\pi}^{\pi} d\phi_1}, \quad (14)$$

which can be simplified as

$$S = \frac{2(\alpha + 1)}{\pi R_T^2 L_1} \int_0^{R_T} dr_1 r_1 \left\{1 - \left(\frac{r_1}{R_T}\right)^2\right\}^\alpha \int_{-L_1/2}^{L_1/2} dz_1 \phi_{max}(r_1, z_1). \quad (15)$$

In contrast to our previous paper [15] above expression contains a non-trivial integration on  $z_1$  coordinate.

Often experimental measurement of  $S$  at given  $N_{part}$  or  $y$  is reported in terms of the  $p_T$  integrated yield ratio (nuclear modification factor) over the range  $(p_T)_{min} \leq p_T \leq (p_T)_{max}$  whose theoretical expression would be

$$\langle S \rangle = \frac{\int_{(p_T)_{min}}^{(p_T)_{max}} dp_T S}{\int_{(p_T)_{min}}^{(p_T)_{max}} dp_T}. \quad (16)$$

So far we have discussed about the suppression of directly produced  $J/\psi$ . However, it is known that only about 60% of the observed  $J/\psi$  originate directly in hard collisions while

30% of them come from the decay of  $\chi_c$  and 10% from the  $\psi'$  [31]. Hence, the  $p_T$  integrated survival probability  $\langle S \rangle$  of  $J/\psi$  in the QGP becomes

$$\langle S \rangle = 0.6 \langle S \rangle_{\psi} + 0.3 \langle S \rangle_{\chi_c} + 0.1 \langle S \rangle_{\psi'}. \quad (17)$$

Now let us turn towards the numerical section of our work where both  $T_D$  sets will be employed.

### 3 Numerical Work

Table 1 gives the values of various parameters used in our theory and the following explanations are relevant in this context. The value  $T_c = 0.17$  GeV is in accordance with the lattice QCD results [1]. The choice  $c_s^2 = 1/3$  is most common for free massless partons in an ideal gas, although for partons which carry thermal mass or interact among themselves,  $c_s^2$  may be different like  $1/5$ . The selection  $\beta = 1$  [16] indicates that the energy deposited in the collision is proportional to the number of nucleon-nucleon collisions. The pressure  $P_s$  corresponding to dissociation temperature is calculated from (6) both for the old [6] and new [7] sets: The entries shown in Table 1 refer to the  $J/\psi$  only for brevity. The initial proper time  $\tau_i$  for QGP thermalization is taken as 0.6 fm/c in accord with our earlier work [15] as well as [36]. Also, relevant properties of the various quarkonia in a thermal medium are displayed in Table 2. It is clear that the dissociation temperature  $T_D$  gradually decreases in going from  $J/\psi$  to  $\chi_c$  to  $\psi'$ .

As regards the length  $L_1$  of the primordial cylinder (in  $c = \hbar = 1$  units) the Lorentz contracted total radius of the Au+Au system gives a very small value  $\sim 2 R_{Au}/200 \sim 0.070$  fm. The alternative estimate based on primordial creation time is also equally small namely,  $\tau_1 \sim 1/2m_c \sim 0.066$  fm/c which, however, can be made more logical by remembering that the corresponding longitudinal locations of the created  $c\bar{c}$  pairs are expected to be of the order  $|z_1| \sim \tau_1 \sinh(|y|)$ . Here  $y$  is the rapidity whose experimentally determined bin reported in PHENIX experiment is  $1.2 \leq |y| \leq 2.2$ . Hence the length  $L_1$  of the cylinder is expected to lie in the range  $0.10 \leq L_1 \leq 0.29$  so that its approximate mid value  $L_1 \sim 0.2$  fm can be used.

Our numerical procedure proceeds through the following steps:

- (i) Before finding the centrality (or impact parameter) dependence of  $J/\psi$  suppression it is necessary to know the initial average energy density  $\langle \epsilon \rangle_i$  in terms of the number of participants  $N_{part}$ . For this purpose, we extract the transverse overlap area  $A_T$  and the pseudo-rapidity distribution  $(dE_T/d\eta_H)_{\eta_H=0}$  reported in ref. [35] at various values of number of participants  $N_{part}$ . These  $(dE_T/d\eta_H)_{\eta_H=0}$  numbers are then multiplied by a constant Jacobian 1.25 to yield the rapidity distribution  $(dE_T/dy_H)_{y_H=0}$  occurring in (5).
- (ii) As regards the choice of the  $\xi$  parameter in (5) two roots are open. In the first root pertaining to the old  $T_D$  values [6] following point is noted. Even though the Bjorken formula provides a qualitatively good estimate of the initial energy density yet, it under-estimates the same, which can cause the suppression of only  $\chi_c$  and  $\psi'$  but not of  $J/\psi$ . Hence, a scaling-up factor  $\xi = 5$  has been introduced in (5) in order to obtain the desired  $\langle \epsilon \rangle_i = 45$  GeV/fm<sup>3</sup> [36] for most central collision. In the second root pertaining to the new set of  $T_D$

Table 1: Various parameters used in the theory

$T_c$ (GeV)	$c_s^2$	$B$ (GeV/fm <sup>3</sup> )	$P_s$ (GeV/fm <sup>3</sup> ) (Old)	$P_s$ (GeV/fm <sup>3</sup> ) (New)	$\beta$	$\alpha$	$\tau_i$ (fm/c)
0.17	1/3	0.405	9.39	0.638	1	0.5	0.60

values [7] the original Bjorken's formula for  $\langle\epsilon\rangle_i$  (without any  $\xi$  parameter) is sufficient to cause the melting of all quarkonia species. The appropriate characterization of kinematic quantities in Au+Au collisions is presented in Table 3 and 4.

(iii) Next, we calculate the time  $\tilde{\tau}_{s0}$  for the pressure to drop to  $P_s$  at the origin and thereby deduce the screening radius  $r_s$  with the help of (8,9,10,11) for  $J/\psi$  mesons of given  $p_T$  and  $y$ .

(iv) Next, the quantity  $Y$  is computed from (12) which sets the condition for the quarkonium to escape from the screening region, and the limiting values of the  $\phi_{max}(r_1, z_1)$  are constructed using equation written just below (12).

(v) Finally, the survival probability  $S$ , at specified  $y$  and fixed  $p_T$  but varying  $N_{part}$  is evaluated by Simpson quadrature using (15) from which  $p_T$  integrated  $\langle S \rangle$  is also deduced.

(vi) The same numerical process is used to calculate the  $\langle S \rangle$  for all other higher quarkonia and finally, by including sequential melting of higher resonances, total  $\langle S \rangle$  has been calculated from (17).

(vii) In order to compare the above analysis with the actual experimental data it is necessary to convert the  $J/\psi$  suppression data available in terms of nuclear modification factor  $R_{AA}$  [12] into the accepted definition of survival probability  $S$  [30, 32] namely

$$S = \frac{R_{AA}}{R_{AA}^{CNM}}, \quad (18)$$

where  $R_{AA}$  is the standard nuclear modification factor and  $R_{AA}^{CNM}$  is a contribution to  $R_{AA}$  originating from CNM effects constrained by the data of  $d + Au$  collisions. The importance of the ratio  $R_{AA}/R_{AA}^{CNM}$  is that it can give direct clue about suppression beyond cold nuclear matter effect, if any. Of course, for a confirmed inference regarding this issue, error bars on the said ratio must be known. For convenience the mathematical expression for the error bar  $\Delta_s$  in  $S$  is recapitulated in the Appendix using individual standard deviation of the numerator and denominator. Unfortunately, the PHENIX experiments [12, 23] do not tell what the correlation coefficient  $r$  between  $R_{AA}$  and  $R_{AA}^{CNM}$  is. Assuming these quantities to be highly positively correlated i.e.,  $r = 1$ , we find

$$\Delta_s = S \left| \frac{\Delta_{R_{AA}}}{R_{AA}} - \frac{\Delta_{R_{AA}^{CNM}}}{R_{AA}^{CNM}} \right|. \quad (19)$$

Now we turn to physical interpretations of our results.



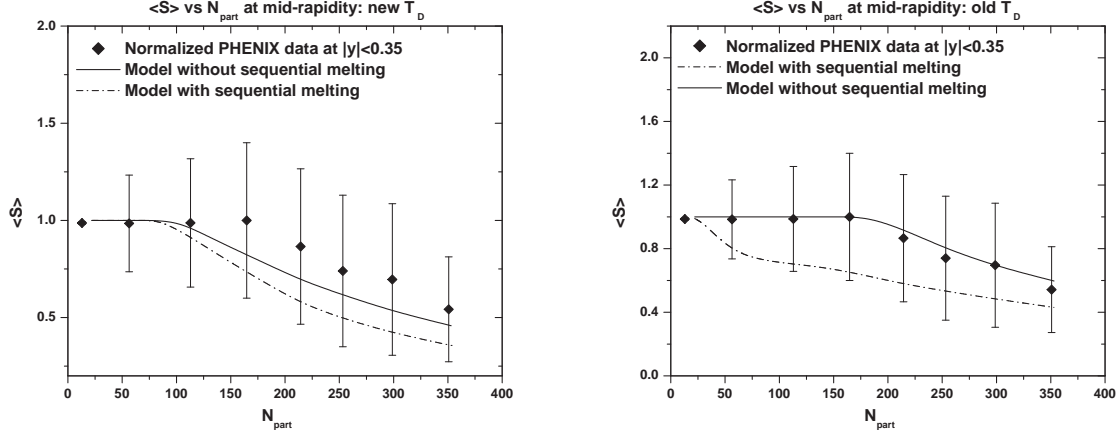


Figure 1: The variation of  $p_T$  integrated survival probability  $\langle S \rangle$  (in the range allowed by invariant  $p_T$  spectrum of  $J/\psi$  measured by PHENIX experiment [12, 23]) versus number of participants  $N_{part}$  at mid-rapidity. The experimental data are shown by solid rhombus with error bars. In the left panel, solid and dash dotted curves represent predictions of our present model without and with sequential melting using new set of  $T_D$  values [7]. In the right panel, same are shown but by using old set of  $T_D$  values [6]. In both Figs.  $\tau_i = 0.6$  fm/c is employed.

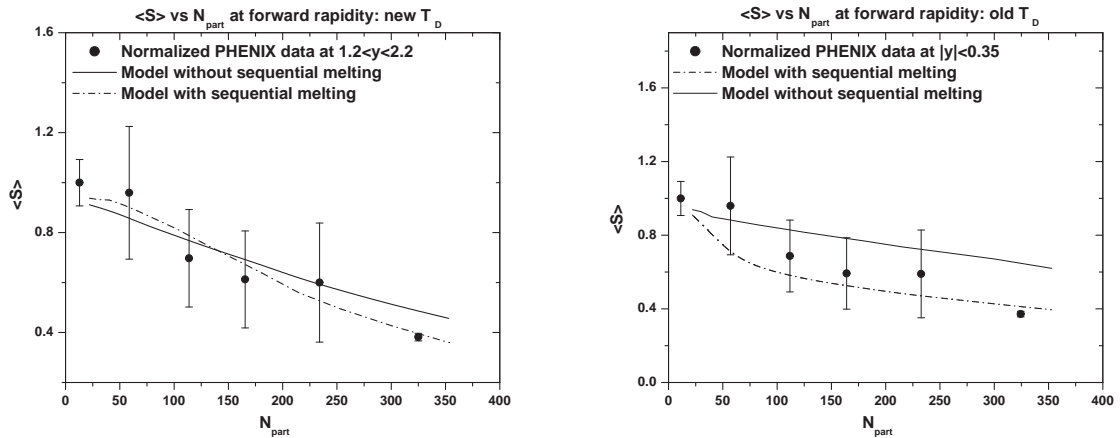


Figure 2: Same as Fig. 1 but at forward rapidity [12, 23].

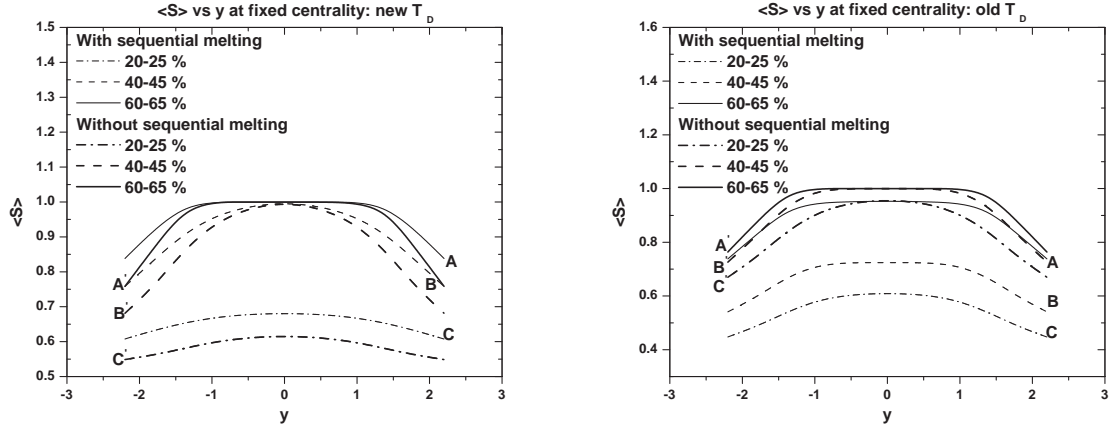


Figure 3: Graph showing the theoretical variation of  $p_T$  integrated survival probability i.e.,  $\langle S \rangle$  with respect to rapidity  $y$  at fixed centralities. Left panel corresponds to the results using new dissociation temperatures for quarkonia [7] with and without sequential melting. Right panel corresponds to the same as in left panel but by using old dissociation temperatures [6].

Table 2: Masses, formation times and dissociation temperatures of  $J/\psi$ ,  $\chi_c$  and  $\psi'$  [6].

	$J/\psi$	$\chi_c$	$\psi'$
$m$ (GeV)	3.1	3.5	3.7
$\tau_F$ (fm)	0.89	2.0	1.5
$T_D/T_c$ (Old)	2.1	1.16	1.12
$T_D/T_c$ (New)	1.2	$\leq 1.0$	$\leq 1.0$

Table 3: Kinematic characterization of Au+Au collisions at RHIC [12] with  $\xi = 5.0$  and  $\tau_i = 0.6$  fm/c in Bjorken's formula when old set of  $T_D$  values [6] is used.

Nuclei	$\sqrt{s_{NN}}$ (GeV)	$\xi$	$N_{part}$	$\langle \epsilon \rangle_i$ (GeV/fm <sup>3</sup> )	$R_T$ (fm)
Au+Au	200	5.0	22.0	5.86	3.45
			30.2	7.92	3.61
			40.2	10.14	3.79
			52.5	12.76	3.96
			66.7	15.69	4.16
			83.3	18.58	4.37
			103.0	21.36	4.61
			125.0	24.38	4.85
			151.0	27.37	5.12
			181.0	30.52	5.38
			215.0	34.17	5.64
			254.0	37.39	5.97
			300.0	41.08	6.31
			353.0	45.09	6.68

Table 4: Kinematic characterization of Au+Au collisions at RHIC [12] without  $\xi$  parameter and with  $\tau_i = 0.6$  fm/c in Bjorken's formula when new set of  $T_D$  [7] values is used.

Nuclei	$\sqrt{s_{NN}}$ (GeV)	$N_{part}$	$\langle \epsilon \rangle_i$ (GeV/fm <sup>3</sup> )	$R_T$ (fm)
Au+Au	200	22.0	1.17	3.45
		30.2	1.58	3.61
		40.2	2.03	3.79
		52.5	2.55	3.96
		66.7	3.14	4.16
		83.3	3.72	4.37
		103.0	4.27	4.61
		125.0	4.88	4.85
		151.0	5.47	5.12
		181.0	6.10	5.38
		215.0	6.83	5.64
		254.0	7.48	5.97
		300.0	8.22	6.31
		353.0	9.02	6.68

## 4 Results and Discussions

We present our numerical results as follows:

Figures 1 and 2 show the variation of  $p_T$  integrated values of the survival probability  $\langle S \rangle$  with respect to number of participants  $N_{part}$  at mid and forward rapidities, respectively. The left and right panels of these figures pertain to the new  $T_D$  set and old  $T_D$  set, respectively. The three curves on each figure correspond to experimental data (solid rhombus) and our model calculation with  $\tau_i = 0.6$  fm/c without sequential melting (solid line) and that with sequential melting (dash dotted line), respectively. It is obvious from the Figures that  $\langle S \rangle$  decreases with increase in  $N_{part}$  both experimentally and theoretically because of the increase in the energy density with respect to  $N_{part}$ . However, it must be emphasized that for the new set of  $T_D$  values [7] (which are all close to  $T_c$ ), the three quarkonia  $\chi_c$ ,  $\psi'$ ,  $J/\psi$  start contributing to  $S$  even at low values of  $N_{part}$ . But for the old set [6] (where  $T_D$  of  $J/\psi$  was about  $2T_c$ ), the contribution of  $J/\psi$  to  $S$  begins only at substantially large  $N_{part}$ . Moreover, within error bars (cf. Figs.1, 2; left panel) the agreement between the experimental data and the prediction of our model is good at mid-rapidity and at forward rapidity provided the new  $T_D$  set is employed without sequential melting. Similarly, the agreement is good (cf. Figs.1, 2; right panel) at mid-rapidity and reasonably good at forward rapidity without sequential melting. However, the agreement becomes poor with old  $T_D$  values particularly at mid-rapidity with sequential melting. A satisfying feature of Figures 1 and 2 is that our model prediction for  $\langle S \rangle$  is obtained by simply inserting the relevant values of the rapidity  $y$  in contrast to other model [29] where different additional parameters are needed for describing the data in different rapidity bins.

However, it must be emphasized in context of Figures 1 and 2 that the physics at mid and forward rapidities has the following important distinctions:

(i) Although the quality of fit between our model and experimental data is good for mid-rapidity data, yet it worsens somewhat for forward rapidity. This may be attributed to the fact that our formulation is based on the assumption of Bjorken's boost invariant longitudinal expansion along the collision axis. This assumption may be violated up to some extent for most forward rapidities.

(ii) As pointed out beneath (11) the radius  $r_s$  of the deadly region at higher rapidity is larger than that at lower rapidities. Therefore, for a  $J/\psi$  meson of given  $p_T$ , the traversal time will also be correspondingly larger implying that the predicted survival probability must decrease with increasing  $|y|$ . This fact is clearly seen in Fig. 3 where we have displayed the variation of  $\langle S \rangle$  with respect to rapidity  $y$  at fixed centrality i.e.,  $N_{part}$  for both  $T_D$  sets. It is clear from this figure that  $\langle S \rangle$  shows peak around  $|y| \approx 0$  and decreases at higher  $|y|$ . This agrees well with the experimental data at RHIC [12, 30, 32].

It should be noted that our model does not involve any free parameter although there are some parameters used in the calculation. We have assigned proper justifications to their values and these values are also used in other calculations e.g., in Chu and Matsui model [16] and hydrodynamical models [30, 36].

At this stage a comment is relevant on the uncertainties in the CNM effects [23] extracted by data-driven method constrained by d+Au collision measurements. In view of

the relatively large error bars in  $R_{AA}^{CNM}$  reported in ref. [23] suggested that it is not possible to make any firm quantitative statements on any additional  $J/\psi$  suppression in Au+Au collisions beyond that expected from cold nuclear matter effects (i.e., due to possible QGP formation). We feel, therefore, that a more firm conclusion about possible QGP formation can be drawn by analyzing results such as Figs.(1-3) if more accurate measurement of both  $R_{AA}$  and  $R_{AA}^{CNM}$  are done in future experiments.

## 5 Summary and Conclusions

Generalization of our previous work [15], based on the  $J/\psi$ +hydro framework involving (1+1)-dimensional expansion of Chu and Matsui [16] model, has been done in the present paper in order to incorporate complete rapidity dependence of the  $J/\psi$  suppression. The present work also takes into account the additional time dilatation effect for charmonium formation due to its motion along general direction and this makes our model different from the calculation by Chaudhari [29] and Gunji et al. [30]. Our formulation shows explicit dependence of the  $J/\psi$  suppression on transverse momentum, centrality as well as on the rapidity and the predictions are consistent with the data. Our model has suitably incorporated the results from recent lattice simulation on the dissociation temperatures [6, 7] and formation time of  $J/\psi$ , as well as on the non-sequential/sequential melting of higher resonances. Using new  $T_D$  values we find that within error bars, the fits predicted by non-sequential and sequential decay modes are both of the same quality with non-sequential one better. We have analyzed the centrality dependence of the  $J/\psi$  suppression data (normalized by contribution due to CNM effects) available from RHIC in terms of the survival probability versus number of participants at mid-rapidity as well as at forward rapidity. Our results reproduce the main feature of the PHENIX data since we observe more suppression at forward rapidity as compared to mid-rapidity region and this is in a good agreement with the recent PHENIX data. It is creditable to notice that the same mechanism explains the suppression patterns observed in the entire rapidity regions. Further extension of this work, such as incorporation of (3+1)-dimensional hydrodynamic expansion and the predictions of our model at LHC energies would provide additional support to our ideas.

In conclusion,  $J/\psi$  suppression is still one of the most potential signatures for deconfinement. Recent PHENIX data on  $J/\psi$  suppression and theoretical Lattice estimates for the dissociation temperatures of  $J/\psi$  family have added more confusions regarding the interpretation of the data. Does a low depletion of  $J/\psi$  yields at RHIC support a much stronger direct  $J/\psi$  suppression (at dissociation temperatures close to  $T_c$ ) and some other mechanism like abundant charm quark production thus creating more  $c\bar{c}$  pairs ? However, more precise data for d+Au collisions are needed to draw a firm conclusion on this issue. We believe that the LHC measurements of  $J/\psi$  yield in Pb+Pb collisions at 5.5 TeV will help in resolving the above confusing issues like sequential screening scenario and dissociation behaviours of  $J/\psi$  and/or  $\Upsilon$  families.

## Acknowledgements

M. Mishra and V. J. Menon are grateful to the Council of Scientific and Industrial Research (CSIR), New Delhi for their financial assistance. C. P. Singh acknowledges the financial support from a research project sanctioned by Department of Science and Technology (DST), New Delhi. We gratefully acknowledge the helpful comments from Dr. Raphaël Granier de Cassagnac on this work. In fact he had suggested us the problem in a private communication.

## References

- [1] T. Hatsuda, J. Phys. G **34**, S287 (2007).
- [2] Z. Fodor and D. Katz, JHEP 0203, 014 (2002); JHEP 0404, 050 (2004).
- [3] F. Karsch, J. Phys. G **30**, S887 (2004).
- [4] T. Matsui and H. Satz, Phys. Lett. B **178**, 416 (1986).
- [5] S. Datta, F. Karsch, P. Petreczky and I. Wetzorke, Phys. Rev. D **69**, 094507 (2004).
- [6] H. Satz, J. Phys. G **32**, R25 (2006).
- [7] A. Mocsy and P. Petreczky, Phys. Rev. Lett. **99**, 211602 (2007).
- [8] M. J. Tannenbaum, Rep. Prog. Phys. **69**, 2005 (2006);  
C. P. Singh, Phys. Rep. **236**, 147 (1993);  
B. Müller and J. L. Nagle, Annu. Rev. Nucl. Part. Sci. **56**, 93 (2006).
- [9] M. C. Abreu et al., Phys. Lett. B **410**, 337 (1997).
- [10] B. Alessandro et al., Eur. Phys. J. C **39**, 335 (2005).
- [11] M. C. Abreu et al., (NA50 Collaboration), Phys. Lett. B **477**, 28 (2000).
- [12] A. Adare et al., (PHENIX Collaboration), Phys. Rev. Lett. **98**, 232301 (2007).
- [13] Xiao-Ming Xu, D. Kharzeev, H. Satz and Xin-Nian Wang, Phys. Rev. C **53**, 3051 (1996).
- [14] B. K. Patra and V. J. Menon, Eur. Phys. J. C **37**, 115 (2004);  
B. K. Patra and V. J. Menon, Eur. Phys. J. C **48**, 207 (2006).
- [15] M. Mishra, C. P. Singh, V. J. Menon and R. K. Dubey, Phys. Lett. B **656**, 45 (2007).
- [16] M. C. Chu and T. Matsui, Phys. Rev. D **37**, 1851 (1988).
- [17] L. Grandchamp, R. Rapp and G. E. Brown, Phys. Rev. Lett. **92**, 212301 (2004).
- [18] A. Andronic, P. Braun-Munzinger, K. Redlich and J. Stachel, Phys. Lett. B **571**, 36 (2003).
- [19] R. L. Thews and M. L. Mangano, Phys. Rev. C **73**, 014904 (2006);  
R. L. Thews, Nucl. Phys. A. **783**, 301 (2007).
- [20] S. S. Adler et al., Phys. Rev. Lett. **96**, 032301 (2006).
- [21] A. Adare et al., Phys. Rev. Lett. **97**, 252002 (2006).
- [22] S. S. Adler et al., (PHENIX Collaboration), Phys. Rev. Lett. **96**, 012304 (2006).
- [23] A. Adare et al., (PHENIX Collaboration), arXiv:0711.3917 [nucl-ex] (2007).

- [24] A. Capella, E. G. Ferreira and A. B. Kaidalov, Phys. Rev. Lett. **85**, 2080 (2000).
- [25] A. P. Kostyuk, M. I. Gorenstein, H. Stöcker and W. Greiner, Phys. Rev. C **68**, 041902(R) (2003).
- [26] M. I. Gorenstein, A. P. Kostyuk, H. Stöcker and W. Greiner, Phys. Lett. B **509**, 277 (2001).
- [27] A. Andronic, P. Braun-Munzinger, K. Redlich and J. Stachel, Phys. Lett B **652**, 259 (2007).
- [28] A. K. Chaudhuri, Phys. Rev. C **74**, 044907 (2006).
- [29] A. K. Chaudhuri, Phys. Lett. B **655**, 241 (2007).
- [30] T. Gunji, H. Hamagaki, T. Hatsuda and T. Hirano, Phys. Rev. C **76**, 051901(R) (2007).
- [31] F. Karsch, D. Kharzeev and H. Satz, Phys. Lett. B **637**, 75 (2006).
- [32] Raphaël Granier de Cassagnac, J. Phys. G **34**, S955 (2007).
- [33] D. Pal, B. K. Patra and D. K. Srivastava, Eur. Phys. J. C **17**, 179 (2000).
- [34] A. Chodos, R. L. Jaffe, K. Johnson, C. B. Thorn and V. F. Weisskopf, Phys. Rev. D **9**, 3471 (1974); K. Johnson, A. Chodos, R. L. Jaffe and C. B. Thorn, Phys. Rev. D **10**, 2599 (1974).
- [35] S. S. Adler et al., (PHENIX Collaboration), Phys. Rev. C **71**, 034908 (2005);  
S. S. Adler et al., (PHENIX Collaboration), Phys. Rev. C **71** 049901(E) (2005).
- [36] T. Hirano, Phys. Rev. C **65**, 011901(R) (2001);  
T. Hirano and K. Tsuda, Phys. Rev. C **66**, 054905 (2002).



## APPENDIX : ERROR BAR CALCULATION IN S (cf.(18))

Let  $a$  be a random variate with mean  $\langle a \rangle$ , fluctuation  $\delta_a = a - \langle a \rangle$ , and standard deviation  $\Delta_a = \langle \delta_a^2 \rangle^{1/2}$ . Similar quantities for another variate  $b$  are called  $\langle b \rangle$ ,  $\delta_b$  and  $\Delta_b$ , respectively. The covariance between  $a$  and  $b$  is denoted by  $C_{ab} = \langle \delta_a \delta_b \rangle = r \Delta_a \Delta_b$  with the correlation coefficient  $r$  lying in the range  $-1 \leq r \leq +1$ . The ratio  $S$  between the variates has the statistical properties

$$S = \frac{a}{b} \quad ; \quad \frac{\delta_s}{S} = \frac{\delta_a}{a} - \frac{\delta_b}{b} \quad (A1)$$

$$\left| \frac{\Delta_S}{S} \right| = \langle (\frac{\delta_S}{S})^2 \rangle^{1/2} = \left\{ \left( \frac{\Delta_a}{a} \right)^2 + \left( \frac{\Delta_b}{b} \right)^2 - 2 \frac{\Delta_a}{a} \frac{\Delta_b}{b} r \right\}^{1/2} \quad (A2)$$

whose special values read

$$\left| \frac{\Delta_S}{S} \right| = \left| \left| \frac{\Delta_a}{a} \right| - \left| \frac{\Delta_b}{b} \right| \right| \quad ; \quad \left| \frac{\Delta_a}{a} \right| + \left| \frac{\Delta_b}{b} \right| \quad ; \quad \left\{ \left( \frac{\Delta_a}{a} \right)^2 + \left( \frac{\Delta_b}{b} \right)^2 \right\}^{1/2} \quad (A3)$$

according as  $r = +1, -1, 0$ , respectively.

In the problem of  $J/\psi$  suppression the error bar formula (19) is obtained by identifying  $a = R_{AA}$ ,  $b = R_{AA}^{CNM}$  and assuming  $r = 1$ .